Passive Wireless UHF RFID Antenna Label for Sensing Dielectric Properties of Aqueous and Organic Liquids

Viktorija Makarovaite, *Student Member, IEEE*, Aaron J. R. Hillier, Simon J. Holder, Campbell W. Gourlay, and John C. Batchelor, *Senior Member, IEEE*

***Abstract*— The *in situ* wireless sensing of dielectric properties for organic aqueous solutions with a wide range of relative permittivities is presented. The use of an ultra-high frequency passive label antenna design attached to either clear borosilicate glass bottle or Petri plate is proposed, which allows for the unobtrusive, safe monitoring of the liquid solutions. The meandered dipole antenna (with a parasitic loop matching component) frequency is highly reliant on the chosen container as well as on the liquid present within, and adjusts with shifting dielectric properties. Tested solutions of high-relative permittivity (such as water) along with low permittivity, lossy liquids (such as xylene) presented distinctive frequency characteristics with read distances of up to 7 m for each type of container tested. The sensor was also able to detect 'unknown' solutions and determine the dielectric properties by utilizing standard curve analysis with an accuracy of ±0.834 relative permittivity and ±0.050 $\mathrm{S \cdot m^{-1}}$ conductivity (compared to a standard dielectric measurement system available on the market). With the accuracy known, tuning the design to fit any necessary frequency is possible as a means to detect specific changes in any one liquid system. This sensor is a possible candidate for discreet real-time monitoring of liquid storage containers and an alternative for low-cost bulk liquid dielectric property identification, which could be implemented in areas requiring, constant, or remote monitoring as needed.**

***Index Terms*— Antenna, battery-free, passive sensing, radio frequency identification (RFID), ultra-high frequency (UHF), wireless sensing.**

I. Introduction

THERE are many industrial chemicals such as butanol and methanol, which produce dangerous vapors equivalent to a category 4 hazard, when opened in enclosed spaces without adequate ventilation [1], [2]. This vapor inhalation can cause common symptoms such as drowsiness, dizziness and respiratory irritation, or with continued exposure can even lead to electrolyte imbalance and kidney failure [1], [2]. Therefore, identifying unknown solutions without the need to open containers and allow vapor formation could be an advantageous application for RFID sensor technology, as well as the capability to determine liquid contamination (or purity) within a closed container autonomously without user interference.

Manuscript received November 5, 2018; revised January 7, 2019; accepted January 16, 2019. Date of publication January 31, 2019; date of current version May 6, 2019. This work was supported by the EPSRC under Project: EP/N009118/1. The associate editor coordinating the review of this paper and approving it for publication was Dr. Ying Zhang. *(Corresponding author: Viktorija Makarovaite.)*

The authors are with the School of Engineering and Digital Arts, University of Kent, Canterbury CT2 7NZ, U.K. (e-mail: vm238@kent.ac.uk).

Digital Object Identifier 10.1109/JSEN.2019.2896481

To address these issues, the sensor proposed here is a low-cost, low-complexity and unobtrusive design, useful for real-time monitoring and *in situ* assessment of liquid solutions such as seen within chemical research and healthcare.

II. Material Sensing Characterization

Material characterization via sensing techniques has rapidly grown within the last decade particularly in the area of low-cost, accurate material analysis and real-time monitoring of samples. Also, polar solutions (molecules with permanent dipole movements) within biomedical applications have been shown to have complex permittivity matching with biological tissues (including medical grade solutions) over the frequency ranges of 300 MHz to 6 GHz [3]. It is known that complex relative permittivity $\varepsilon^* = \varepsilon' - \mathrm{j}\varepsilon''$, (where ε' is its real part, ε'' is the imaginary part and $\tan\delta = \varepsilon''/\varepsilon'$ is the loss tangent) has a strong frequency dependence due to molecular dielectric relaxation behavior [3]. In biomedical measurements such as Specific Absorption Rate (SAR), material loss can be expressed in terms of equivalent conductivity, σ; where $\sigma = 2\pi f \varepsilon'' \varepsilon_0$ with f being frequency and ε_0 free space permittivity [3].

The high dependence of these organic solutions on frequency provides a mechanism for dielectric liquid identification when using electrically small antenna designs, which can be easily tuned to a lower frequency range via a high dielectric backing [4], [5]. However, this frequency shift is highly dependent on not only the dielectric properties but also the thickness of the backing. Therefore, it is possible to normalize solutions to reduce the effect of conductivity and permittivity for liquid differentiation [6]. This can be seen in the use of (1) for determining effective permittivity:

$$\varepsilon_{eff} = \varepsilon_0 (f_0{}^2 / f_{\mathrm{over}}{}^2) \tag{1}$$

where f_0 was the starting frequency and f_{over} is the resulting changed frequency after the addition of the polar solution [6], [7]. However, this equation is not applicable if dielectric thickness is not maintained at a constant level, meaning that thickness variation in the walls of each container (or reservoir) will skew the results [6], [7].

Organic solution identification and antenna design has been previously reviewed, and sensors exist to detect these solutions [3], [5], [8]–[11]. However, a single chipped design capable of identifying both polar and non-polar (no-dipole

moment, low relative permittivity ($\varepsilon_r' = 2 - 11$) and low loss ($\tan \delta < 0.001$)) organic solutions, and spanning a range of relative permittivities, is not available due to the large variability in solution dielectric properties. Additionally, most of the current published designs for any RFID based dielectric sensing are not only incapable of testing both low and high dielectric solutions but, also, are all chipless systems functioning above 1 GHz with most requiring a minimum frequency span of 500 MHz to differentiate their limited solution dielectric ranges [3], [5], [8]–[11]. The present approach attempts to provide such a sensor capable of detecting and differentiating an assortment of organic liquids with dielectric constants ranging from 2 to 80 within a single design and within less than 200 MHz frequency span for research use.

III. Methods

The basic principle of operation requires the excitation of a resonant mode within a known container, where the resonant frequency is dependent on the liquid present within the chosen container [3], [5]. The sensor is excited wirelessly via a reader antenna, and a calibrated Voyantic TagformancePro system [12] detects the resonant frequency. Specifically, the TagformancePro system ramps power up to a set max (30dBm) and stops transmission once a signal is received back to the system (correlating output to the transmitted power levels); the links for this type of system are forward power limited.

The proposed antenna label assumes a full chosen container filled to a known level (100 mL in an 80 mm diameter borosilicate glass bottle and 20 mL in a 100 mm diameter borosilicate glass petri dish) rather than a very minute sample as seen with other systems [3]. Presenting a highly lossy environment, allowing the polarity of the system to correlate with the shift in the frequency for a known thickness (fill level) of the dielectric used. This easy attachment and reading of the liquid can be affected by a change in the dielectric properties of the solution in question allowing for identification of the dielectric properties (once plotted) against known solutions of the same quantity.

A. Antenna Design

A Higgs-3 Electronic Product Code Class 1 Gen 2 RFID integrated circuit (IC) ($Z_C = 23 - \mathrm{j}192\ \Omega$ at 920 MHz) [13] was matched to a copper etched meandered dipole antenna (Fig. 1), by utilizing a matching resonating loop system.

In any RFID design, the impedance of the antenna (Z_A) must be conjugate matched to Z_C. Antenna placement on any material other than air will require either compensation or antenna retuning. When compensating for this change in antenna impedance, shunt scaling [14] can be utilized as an impedance matching network.

Shunt scaling uses the approach that if a reactance (X_p) is placed in parallel (shunt) with a known antenna impedance (Z_A), then Z_A can be expressed as:

$$Z_{\mathrm{A}} = \frac{R_C \cdot {X_p}^2}{{R_C}^2 + \left(X_C + X_p\right)^2} + \mathrm{j}\frac{X_p \cdot \left[{R_C}^2 + X_C \cdot \left(X_C + X_p\right)\right]}{\left({R_C}^2 + \left[X_C + X_p\right]^2\right)} \quad (2)$$

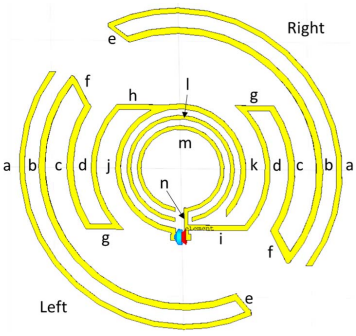

	Length (mm)		Length (mm)
a	36	**h**	5
b	33	**i**	6
c	12	**j**	13
d	12.5	**k**	13.5
e	3.3	**l**	23
f	3.7	**m**	20
g	3.5	**n**	2

Fig. 1. Liquid sensing UHF RFID half wave dipole antenna design with a 29 mm diameter and a parasitic loop matching system with three conductor widths: 1) 0.5 mm for lengths a - c and e - g; 2) 0.4 mm for lengths d, h - k; and 3) 0.3 mm for l - n.

where R_C and X_C are respectively the real and imaginary parts of Z_C. Given that $Z_A = R_A + \mathrm{j}X_A$, shunt scaling for resistance [14] was used to develop a matching loop system with an alpha scalar ($\alpha = R_A/R_C$) of 0.29 when the antenna, Mylar and petri glass container have a combined impedance of $Z_A = 6.74 - \mathrm{j}131.9\ \Omega$ such that $R_A = R_{tag} + R_{glass} + R_{mylar}$ and $X_A = X_{tag} + X_{glass} + X_{mylar}$). It was shown in [14] that when the reactance of the IC is negative ($X_C < 0$), either a shunt capacitance 0.81 pF or a shunt inductance of 1.3 nH will satisfy (3) for $\alpha = 0.29$.

$$X_p = \mp\frac{\sqrt{\alpha}}{1 \pm \sqrt{\alpha}} \cdot X_C \quad (3)$$

A shunt capacitance was chosen due to its linear frequency dependence. This led to a highly meandered half-wave dipole and a 1 pF capacitive loop system of about 29 mm in diameter (Fig. 1). Altogether, the two meandered dipole sides had lengths of 122 mm (left) and 110 mm (right), more than enough to account for the needed length for a half-wave dipole at 920 MHz.

B. Antenna Placement

The antenna label was attached to achieve the optimal matching with the container(s) chosen [12]. For the petri dish attachment, the sensor was placed on the underside of the 100 mm diameter borosilicate glass petri dish, Fig. 2 (A). It is important to note that the borosilicate glass had a 2 mm thickness and a glass height of 12 mm. A 500 mL borosilicate glass bottle (80 mm diameter) with a 5 mm glass thickness was also tested to determine the role of glass and liquid thickness on the sensor sensitivity, Fig. 2 (A).

The TagformancePro system was arranged as indicated in Fig. 2 (C) with a calibrated 30 cm space between the reader antenna and the sensor tag attached to the solution container. The configuration was set to a 'transmitted power' sweep between 750 MHz to 1000 MHz (for the petri dish) and 800 MHz to 1000 MHz (for the bottle) with 5 MHz frequency and 0.1 dBm power steps (up to 30 dBm) to identify any shifts in resonance to allow for effective permittivity calculation in (1).

C. Simulation

CST software suite is a time domain based electromagnetic simulator able to model material parameters in three

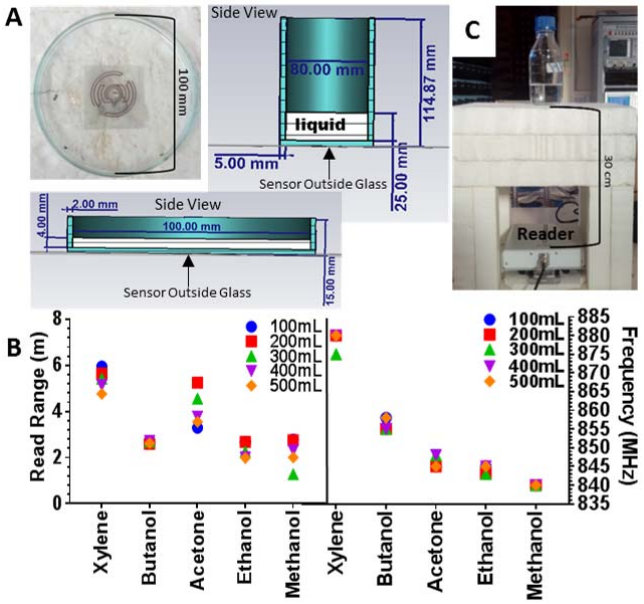

Fig. 2. Experimental setup. (A) Top view of antenna sensor placement on a borosilicate glass petri plate, and diagram of antenna placement of petri and bottle in side view (from CST simulation software). (B) Read range and frequency affect with change in volume within bottle. (C) Voyantic TagformancePro system arrangement with a 30 cm space between the reader antenna and the sensor on the bottom of either the borosilicate bottle or petri plate (bottle procedure shown).

dimensions [15]. For CST simulation purposes, the borosilicate glass properties were set as 7 for permittivity and $1 \times 10^{-11} \mathrm{S \cdot m^{-1}}$ conductivity. Mylar thickness was calculated as 0.13 mm with a permittivity of 3.6 and conductivity of 0.0004 $\mathrm{S \cdot m^{-1}}$. As previously stated, the petri dish was modelled with a 100 mm diameter and 2 mm glass thickness with a liquid layer of 4 mm in height (equivalent to 20 mL of solution) (Fig. 2 (A)). The glass bottle was modelled as a cylinder with an 80 mm diameter and 5 mm wall thickness. For the liquid level equal to 100 mL of solution, a layer of 25 mm was simulated within the 115mm cylinder (Fig. 2 (A)). The simulated read distances (using built in CST capabilities) were calculated at the peak resonant frequency for each organic liquid tested, the receiver sensitivity was set at −20 dBm with a chip capacitance and impedance based on the Higgs-3 SOT IC [13] for the needed resonant frequency. This simulation sensitivity was chosen as (based on empiral experimentation) this provided a good working minimum read distance estimation without over estimation. All the simulated organic solution dielectric properties were taken from Table I and Table II. The simulated resonant frequency responses for each liquid type and estimated read distance are shown in Fig. 3 (A) for the pertri dish and (B) for the bottle, and compared to the measured results.

It should be noted that there is no air gap between the glass and the RFID tag as the tag is directly attached onto borosilicate glass by very thin (<5 micron) adhesive layer when measured (this adhesive layer was not included in simulation as the layer thickness was not electrically significant). As tag placement variability is possible even on the standard laboratory bottles and petri dishes utilized here, a future standard procedure must be defined for sensor placement.

TABLE I

DIELECTRIC PROPERTIES OF THE SIX POLAR LIQUIDS USED WITHIN THE EXPERIMENT

Liquid	*Permittivity (294.13K)*	*Conductivity S/m*	*Petri Effective Permittivity*	*Bottle Effective Permittivity*
DI Water	78.20±0.20	0.09	1.462	1.196
Methanol	30.88±0.27	0.38	1.317	1.140
Ethanol	14.53±0.47	0.54	1.227	1.126
Acetone	21.10±0.30	0.07	1.227	1.126
1-Butanol	4.75±0.34	0.22	1.118	1.087
Xylene	2.57±0.15	0.07	1.080	1.027
Air	1	0	1	1

TABLE II

EXPERIMENTAL EFFECTIVE PERMITTIVITY FOR A RANGE OF ETHANOL SOLUTIONS

	Permittivity (297.45K)	*Conductivity (S/m)*	*Petri Effective Permittivity*
Water	77.8	0.169	1.426
25% Ethanol	64.6	0.283	1.389
50% Ethanol	48.9	0.35	1.337
75% Ethanol	33.6	0.427	1.320
100% Ethanol	16.2	0.483	1.213
	Permittivity (299.15K)	*Conductivity (S/m)*	*Petri Effective Permittivity*
100% Xylene	2.4	0.023	1.068
75% Xylene	4.9	0.096	1.068
50% Xylene	7.8	0.225	1.17
25% Xylene	11.1	0.372	1.18

D. Liquids

Six common organic liquids with relative permittivities ranging from 2 to 80 were chosen for determining the effectiveness of the antenna label sensor as a liquid identification system. These liquids have been studied within the antenna sensor field and their dielectric information is readily available [3], [5]. The six tested liquids were methanol, ethanol, butanol, acetone, xylene and deionized (DI) water. From experimentation, it was determined that 100 mL of solution in the 500 mL bottle presented the optimal results for differentiating various liquid chemicals. However any chemical amount up to 500 mL can be utilized for differentiation showing a discreet effective permittivity for each type of chemical.

Finally, to get a standard calibration curve for a permittivity range of 2 to 80, varying percentages of ethanol to DI water, as well as xylene to ethanol were used (Figs. 5 to 8). This allowed for a more accurate representation of how a standardized level change in permittivity affects the solution resonance frequency and effective permittivity. These standardized DI solutions were 100%, 75%, 50% and 25% percent ethanol (and

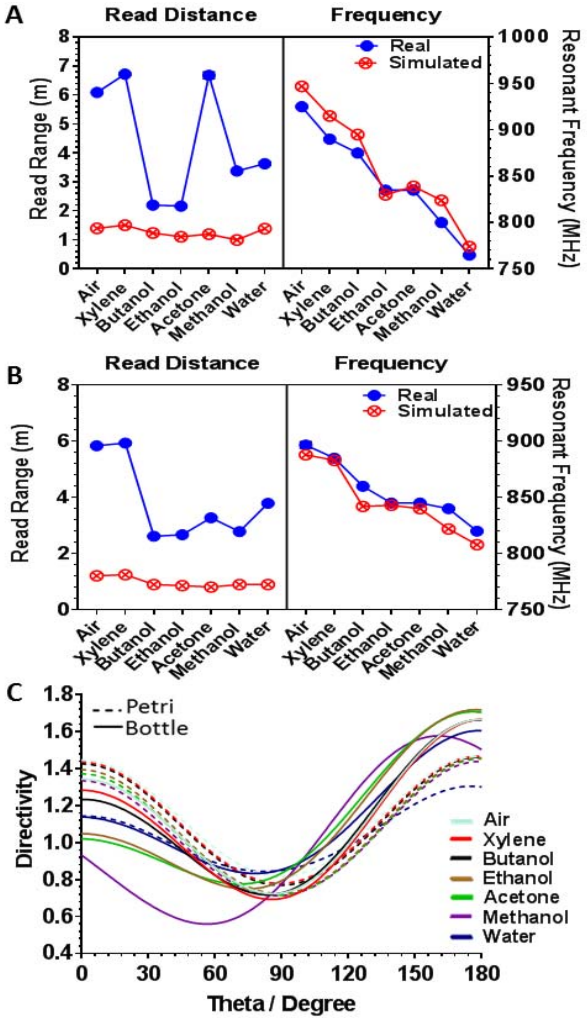

Fig. 3. Resonant frequency for the tested polar solutions within a borosilicate glass (A) petri dish and (B) bottle. Simulated and real resonant frequency readings had a good match for the chemicals tested; however, the read distance was underestimated for the simulated results compared to the real results. Real results showed no deviation between repeats with the highest read distances presenting for air, xylene and acetone in the petri setup and only air and xylene for the bottle setup (n = 3). Simulated results for water were averaged between the two observed resonant peaks in bottle (B) simulation only as all other simulations produced the same single resonance peak with multiple repeats. C) Simulated farfield directivity cut at phi 90° for each liquid tested at resonance with linear scaling for both petri and bottle settings. Theta 0° and 180° represent main vertical beam.

the same percentages were used for xylene solutions mixed with ethanol). The liquid solutions were named as to reflect the percentage of ethanol in each solution, for example: 25% ethanol = 25% ethanol to 75% DI water, while 25% xylene = 25% xylene to 75% ethanol. The same naming trend was utilized for all the solutions. All liquid dielectric properties were measured at 865 MHz using a SPEAG Dak 3.5 probe [16] with a Rohde and Schwarz ZVL 6 GHz network analyzer using the standard manufacturer recommended procedure [15]. The measured values are given in Table I.

E. Single Frequency

After determining the sensitivity of the presented sensor, the sensors design can be tuned within any licensed EPC band to allow for easy UHF RFID liquid identification utilizing a single RFID reader without the requirement of any research quality wideband readers (as needed in previous sections). This would involve a simple adjustment to the dipole lengths. The design was tuned using parameter sweeps with CST software to determine the ideal dipole lengths for each frequency tested; calculated for 867 MHz and 920 MHz for both petri and bottle (Table IV). The results are given as left and right dipole lengths based on Fig. 1 overall side lengths.

F. Repeatability

To check the repeatability and accuracy of each liquid resonant frequency reading, an empty 'air' standard was run between each new replicate for every liquid tested as well as when switching between the different types of organic liquids. No noticeable resonant frequency drifts occurred throughout the experiment as each organic liquid readings were repeated in triplicate within multiple days. However, as the measurements were completed within a few weeks, it is possible that a frequency drift could occur with continued use. Therefore, all readings should be verified by the inclusion and tracking of an 'air' standard for any system utilizing this passive UHF liquid sensing system.

IV. Results and Discussion

When measured with the Voyantic system, each organic liquid demonstrated a distinct resonant frequency in both the 2 mm thick walled petri dish, Fig. 4 (A) and the 500 mL borosilicate glass 5 mm thick walled bottle, Fig. 4 (B). There was a wider resonance separation in accordance with the effective permittivity for the thinner petri plate than the thicker bottle yet the overall trends remained the same. Empty containers had the highest resonance frequency whereas ethanol, acetone, and methanol showed a downward shift. Both container types had more difficulty differentiating between the alcohol solutions as these had very similar dielectric properties. However, as previously seen with the resonant frequencies, the overall trend in effective permittivity is identical between the two systems (Table I). Also, it should be noted that testing volume levels from 100 mL to 500 mL produced at most a 5 MHz resonant frequency shift for each organic liquid tested, Fig. 2 (B). Specifically, acetone produced a resonant frequency range from 845 MHz to 850 MHz (Fig. 2 (B)). Butanol and xylene also had resonant frequency shifts of 5 MHz; butanol ranged from 860 MHz to 865 MHz while xylene ranged from 880 MHz to 885 MHz (Fig. 2 (B)). Ethanol, methanol and DI water, however, remained unchanged and produced a constant resonant frequency from 100 mL to 500 mL volume of liquid (Fig. 2 (B)). However, it should be noted that with the increase above 100 mL, there was a change in read range for most of the organic liquids at their resonant frequency (Fig. 2 (B)). Though all read distances remained above 1 meter (at a minimum) throughout all the volumes tested (Fig. 2 (B)). For the petri dish, 20 mL of solution was used as the standard amount as this provided optimal repeatable results.

Finally, to verify the modulated signal resonance (S11), a loop coupling method with a network analyzer was utilized for both air readings Figs. 4 (C) and (D). This showed that

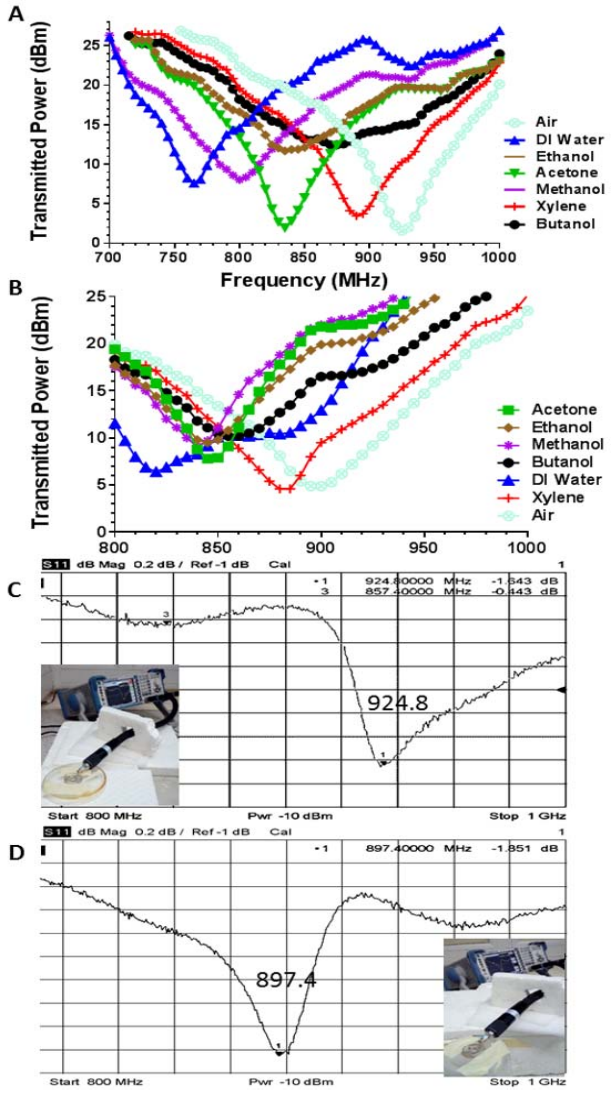

Fig. 4. Transmitted power for the tested polar solutions within A) 2 mm thick borosilicate glass petri dish and B) 5 mm thick borosilicate glass bottle. As permittivity increases, a downward shift in resonance occurs as expected. The three replicates for each chemical had no deviation (n = 3). (C) Petri and (D) bottle: S11 check for resonance without a modulated signal (in air) using a 2 cm loop coupled system with a ZVL Rhode & Schwarz network analyzer.

both the TagformancePro and ZVL Rohde & Schwarz 6 GHz network analyzer produced the same resonant frequency for the air standards at 897 MHz (bottle) and 925 MHz (petri). Overall, the results exhibited the expected trends for increasing permittivity leading to a downward shift in resonance frequency.

A. Measured Resonance Shifts

The sensor match on the petri dish was achieved at a resonant frequency for air from 920 to 925 MHz with a bandwidth of about 100 MHz (transmitted power equal to or smaller than 15 dBm) equivalent to read range of 6.1 m when measured on the TagformancePro reader. For the bottle, the same resonance shift trend was seen. These results were as expected based on simulations as seen within Figs. 3 (A) and (B). The measured resonant frequency of the empty bottle also matched the desired frequency band at 915 to 925 MHz, resonating at 900 MHz with an acceptable bandwidth of about 100 MHz.

The loss in sensor sensitivity for the increased glass thickness in the bottle suggests that the material effect of the glass was overestimated by CST simulation when matched to air (Figs. 3 (A) and (B)). Due to the circular and parasitic nature of the antenna design, the electric fields add in phase rather than cancel leading to increased material penetration by the fields than modeled. This would also explain why the simulated read ranges were a fraction of the distances measured by the TagformancePro reader, Figs. 3 (A) and (B). When looking at directivity, the sensor design had a unidirectional appearance, with theta at both 0° and 180° representing the vertical main beam directions.

B. Measured Resonance Shifts

The sensor match on the petri dish was achieved at a resonant frequency for air from 920 to 925 MHz with a bandwidth of about 100 MHz (transmitted power equal to or smaller than 15 dBm) equivalent to read range of 6.1 m when measured on the TagformancePro reader. For the bottle, the same resonance shift trend was seen. These results were as expected based on simulations as seen within Figs. 3 (A) and (B). The measured resonant frequency of the empty bottle also matched the desired frequency band at 915 to 925 MHz, resonating at 900 MHz with an acceptable bandwidth of about 100 MHz.

The loss in sensor sensitivity for the increased glass thickness in the bottle suggests that the material effect of the glass was overestimated by CST simulation when matched to air (Figs. 3 (A) and (B)). Due to the circular and parasitic nature of the antenna design, the electric fields add in phase rather than cancel leading to increased material penetration by the fields than modeled. This would also explain why the simulated read ranges were a fraction of the distances measured by the TagformancePro reader, Figs. 3 (A) and (B).

The resonance frequencies of each organic solution encompassed read ranges between 7 to 2 m for the petri dish, Fig. 3 (A), and 6 to 3 m for the bottle, Fig. 3 (B), dependent on the chemical used. This suggests that this sensor design is suited for use on glass containers. Air and xylene provided the longest read ranges for both glass containers (around 6 m for both in the bottle, and 6.1 and 6.7 m respectively for air and xylene in the petri dish). Xylene is a low polarity viscous fluid with a low conductivity (400 $\mathrm{pS} \cdot \mathrm{m}^{-1}$) and relative permittivity (2.6) [17], and able to cause a 35 MHz downward shift compared to air (permittivity 1 and conductivity 0.008 $\mathrm{pS} \cdot \mathrm{m}^{-1}$) while increasing the read distance of the tag, Figs. 4 (A) and 3 (A). Also, for the petri measurement, acetone showed a read range above 6.5 m.

The overall trends between the calculated effective permittivities were identical between both sensor tag applications with a slight increase in sensitivity within the petri plate system allowing for a more distinct chemical identification when only using effective permittivity (Table I). Based on the results, increased glass thickness seems to decouple the liquid from the sensor enough to reduce the sensitivity of the sensor. This is most noticeable between the alcohols as

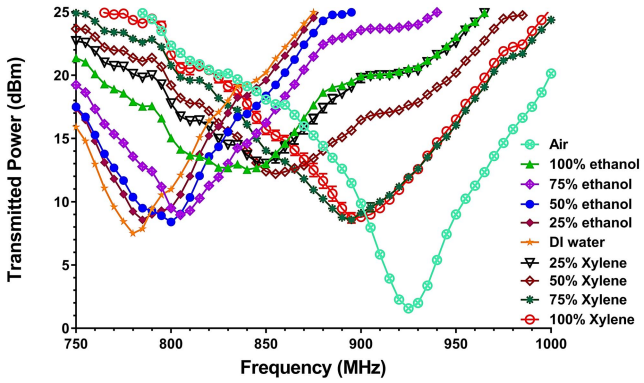

Fig. 5. Measurement of ethanol calibration solutions within a 2 mm thick borosilicate glass petri dish (three replicates each). There was some deviation within the replicates seen with 100% xylene and 25% xylene; however, the variance did not change the resonant frequencies just affected the transmitted power levels. There was a downward shift with increasing permittivity and less variance between solutions of close conductivity. Only 75% xylene and 100% xylene were indistinguishable from each other, all other solution mixes had unique resonance points.

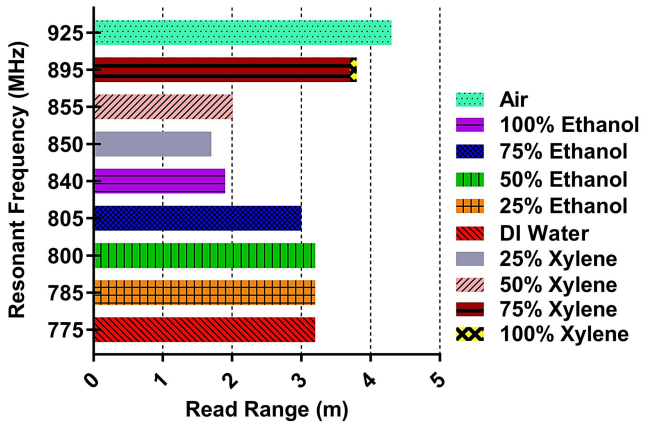

Fig. 6. Measure resonant frequency for the tested ethanol mixtures within a borosilicate glass petri dish. The read range showed between 2 m to about 4 m. The highest read distances were seen with 'air' at 4.3 m and both 100% and 75% xylene solutions about 3.8 m.

there is a much smaller resonance difference between butanol, ethanol/acetone and methanol within the glass bottle, than for the petri dish. For example, the tag on butanol resonates at 875 MHz while methanol resonates at 800 MHz within the petri dish, whereas in the bottle the same solutions resonate at 860 MHz and 840 MHz respectively, Figs. 3 (A) and (B). That is a difference of 75 MHz versus 20 MHz for the same solutions.

C. Standardization of Ethanol Solutions

Ethanol solutions were utilized to achieve a standard curve for identifying solution properties based on the effective permittivity and to determine the relationship between the standard dielectric properties and effective permittivity. The petri dish set-up was utilized as it exhibited more sensitivity as seen in Section IV (A). There is a large difference between the air, 100% ethanol and DI water measurements (Fig. 5); however, the measurements between 75% ethanol and 25% ethanol become more difficult to differentiate as the values clustered around an effective permittivity of 1.3 (Table II). The resonance frequencies showed sensor tag read distances between 2 and 4 m with most of the samples giving around 3 m (Fig. 6).

There is an adequate variability between the permittivities within these close values but the conductivity does not show such a high variability (Table II and Fig. 7). It should be noted that conductivity affects resonance; however, it is primarily dependent on relative permittivity as it cannot affect a change alone within an acceptable correlation margin. Excluding air, the highest conductivity variance (with a relative low change in permittivity) stepwise is seen between DI water and 25% ethanol with a change of 0.114 $S \cdot m^{-1}$ causing only 10 MHz shift, whereas, a conductivity change of 0.053 $S \cdot m^{-1}$ between 100% and 75% ethanol showed a shift of 35 MHz. For the same calibration steps, even if conductivity only decreases by 0.053 $S \cdot m^{-1}$, the permittivity doubles leading to a more substantial downward frequency shift.

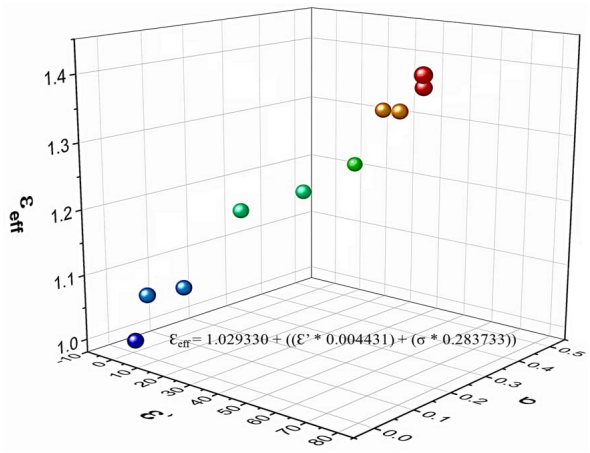

Fig. 7. XYZ plot of dielectric properties of the ethanol calibration solutions used within the experiment for the glass petri plate with 20 mL of each solutions from Table II. Comparison of calculated effective permittivity and measured standard permittivity and conductivity of solutions. A multivariate regression was used to determine the relationship between the effective permittivity and the relative permittivity and conductivity. Both conductivity (σ) and relative permittivity (ε') affect effective permittivity (ε_{eff}). The adjusted R-square value showed a correlation of 0.97 with a high significance (2.24e-6).

In order to make a complete permittivity curve, xylene was also mixed with ethanol (rather than DI water) to reduce the relative permittivity below that of absolute ethanol. Permittivity ranged from 2.4 to around 16, whereas conductivity varied from around 0.02 to 0.5 $S \cdot m^{-1}$ (Fig. 6). This further indicates that relative permittivity plays a primary role in frequency shifts than conductivity alone as 50% ethanol and 25% xylene both have similar conductivities (0.35 and 0.37 $S \cdot m^{-1}$, respectively), yet had a resonant frequency shift of 50 MHz owing to a relative permittivity difference of more than 30.

Also, comparing effective permittivity only against measured conductivities with simple linear regression for all the ethanol standardization solutions, they produced no significant differences (p value >0.05 and $R^2 = 0.168$). However, when conductivity was included in the calculations alongside relative permittivity, a strong relationship was noted with effective permittivity, Fig. 7. This led to the creation of an equation for

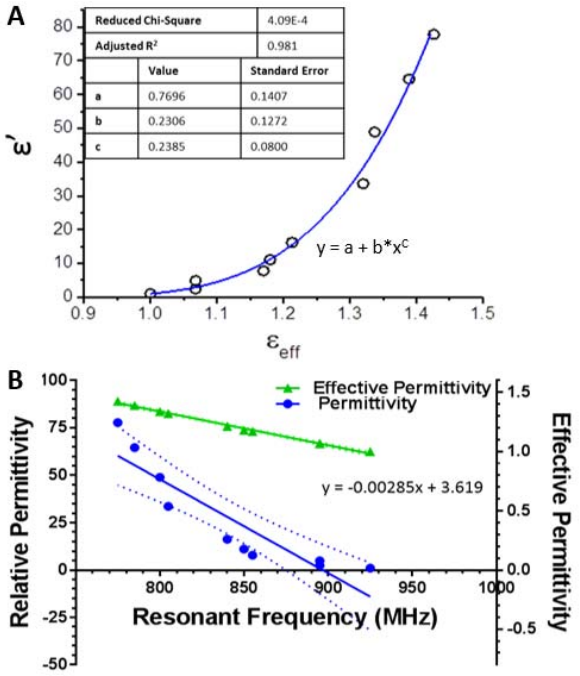

Fig. 8. (A) The relationship between effective permittivity and relative permittivity. No linear relationship exists, but by using an allometric model, there exist a power relationship where 'x' (relative permittivity) is proportional to 'y' (effective permittivity), when 'x' is set to a power 'c' multiplied by 'b' and combined with 'a'; a significant R^2 value of 0.981 is shown. (B) Standard curve of effective permittivity and relative permittivity against resonant frequency. Calculated effective permittivity exhibits a clear linear relationship with resonant frequency (p value < 0.05; $R^2 = 0.994$) while the relationship between measured relative permittivity and resonant frequency alone is not significant (p value > 0.05; $R^2 = 0.825$). Included equation corresponds with a linear regression for effective permittivity to help interpolate unknown samples.

ε_{eff} relating ε' and σ obtained from a multivariate regression analysis and shown in Fig. 7.

As noted, relative permittivity and conductivity both simultaneously affect tag resonance on chemical solutions (as these values are known to be frequency dependent) especially when using a single type of sensor design. Thus, effective permittivity could be a better (or equivalent) identifier for chemical solutions than dielectric constant alone as it normalizes all the outside factors other than the chemical composition allowing for a single measurement using a UHF RFID reader only.

D. Interpolation of "Unknowns"

There is a clear differentiation between the standardization mixtures (Fig. 6) particularly when comparing relative permittivity or effective permittivity against resonant frequency (Fig. 8). In this instance, relative permittivity with linear regression produces an R^2 value of 0.825 while effective permittivity gives an R^2 value of 0.994 (Fig. 8). This shows that resonant frequency only has an acceptable correlation with effective permittivity and not relative permittivity on its own. All three curve fit equations plotted in Figs. 7 and 8 allow for the determination of dielectric properties of a solution from only the calculated effective permittivity without the need for additional equipment other than a UHF RFID reader.

It is possible to estimate an unknown solution's dielectric properties and resonant frequency by using the effective permittivity standard curve presented in this paper, (Figs. 7 and 8 (A)). To examine this, all the solutions in Table I were re-measured due to the increase in ambient temperature (294.13K to 297.45K) as temperature is known to affect dielectric properties [18]. This led to a slight shift in the effective permittivities for solutions in Table I (referred to as the "unknowns" for comparison reasons). The values in Table III indicate that the system was affected by the change in temperature between the two reading sets as expected. However, the correlation between the standard dielectric testing system (SPEAG Dak 3.5 probe system) and the presented sensor design showed high accuracy. It is expected that dielectric properties would change with temperature that is why all dielectric measuring equipment (such as the SPEAG Dak system) available on the market require a calibration step for temperature.

For example, butanol shows an effective permittivity (ε_{eff}) of 1.131, making the dielectric properties between 75% and 50% xylene (Table II). By utilizing the equations plotted in Figs. 7 and 8, it is possible to produce a calculated relative permittivity of 6.55 and calculated conductivity of 0.26 $S{\cdot}m^{-1}$. This is within 0.26 of the measured permittivity (ε'_m) and 0.04 $S \cdot m^{-1}$ of the measured conductivity (σ_m) of the butanol values measured at 297.45K (Table III). Also, it should be noted that with the change in temperature, acetone ($\varepsilon_{eff} = 1.253$) and ethanol ($\varepsilon_{eff} = 1.238$) were distinguishable from each other. By repeating this for all the other measured liquid dielectric and resonance values within Table I, it is possible to determine that the current system (when using only effective permittivity) has a calculated accuracy of ± 0.834 relative permittivity and ± 0.050 $S \cdot m^{-1}$ conductivity when looking at the correlation between the standard Dak dielectric measurement probe system and the presented sensor design.

It should be noted that acetone values were excluded for the conductivity calculation of the mean absolute deviation (MAD) as the proposed system cannot differentiation below a conductivity of 0.096 $S \cdot m^{-1}$ as seen with the lack of differentiation between 75% and 100% xylene standards. The same was done for permittivity values where methanol was excluded due to being an outlier but if methanol values were included then the average deviation would still only be within ± 2.2 relative permittivity; this is equivalent to an R^2 value difference of 0.9997 versus 0.986 (respectively) with linear regression analysis.

E. Single Frequency

As this design is ultimately a dipole antenna, it is easily tunable to fit any chemical by a simple tuning approach. Also, due to this design's sensitivity to minute changes in dielectric properties, it could potentially be used to detect chemical contamination within these closed glass systems as in Fig. 5 (ethanol was diluted with DI water). Therefore, it should be possible to utilize a single UHF frequency by adjusting the dipole lengths of this design to fit any regional frequency regulations for UHF antennas. Table IV shows just such changes needed to match the frequencies within either the ETSI or FCC EPC Class 1 Gen 2 ISO18000-6C RFID requirements. In the future this could allow for any chemical to be tested

TABLE III

DIELECTRIC PROPERTIES OF THE SIX "UNKNOWN" LIQUIDS USED WITHIN THE EXPERIMENT (297.45K)

Liquid	ε'_m	σ_m *(S/m)*	ε_{eff}	*Calc.* ε'	*Calc.* σ *(S/m)*	*Error* ε'	*Error* σ *(S/m)*
DI Water	77.8 ± 0.09	0.169	1.426	80.44	0.142	+2.64	-0.027
Methanol	31.5 ± 0.24	0.38 ± 0.02	1.327	40.43	0.418	+8.93[a]	+0.038
Ethanol	16.2 ± 0.19	0.483 ± 0.001	1.213	15.52	0.405	-0.680	-0.078
Acetone	22.39 ± 0.05	0.055 ± 0.001	1.253	22.30	0.440	-0.090	+0.385[a]
1-Butanol	6.29 ± 0.007	0.218 ± 0.001	1.131	6.55	0.255	-0.260	+0.037
Xylene	3.5 ± 0.23	0.16 ± 0.001	1.068	3.00	0.094	-0.500	-0.066
Air	1	0	1	x	x	x	x
Mean Absolute Deviation (MAD)	x	x	x	x	x	0.834	0.05

Calculated dielectric properties from effective permittivity in comparison to SPEAG Dak system measured values. Read with the Dak system at 860 MHz frequency. Symbol 'a' shows outliers excluded from MAD calculation.

TABLE IV

CST SOFTWARE SIMULATED DIPOLE TUNING

Type	Bottle				Petri			
	ETSI 865.6 - 867.6 MHz		FCC 902 – 928 MHz		ETSI 865.6 -867.6 MHz		FCC 902 – 928 MHz	
	Right	*Left*	*Right*	*Left*	*Right*	*Left*	*Right*	*Left*
Air	108	120	X	X	110	122	X	X
Acetone Ethanol	94	106	82	94	93	105	85	97
Methanol	92	104	80	92	90	102	80	92
Butanol	X	X	85	97	X	X	90	102
Xylene	102	114	94	106	105	117	95	107
Water	78	90	70	82	72	84	66	78

CST simulation adjusted lengths (mm) of each dipole side to fit a single UHF RFID reader within the EPC 18000-6C RFID regulations. The 'X' notes chemicals that do not require any additional tag tuning to fit suggested frequency band.

for contamination or purity within a closed bottled system as long as the tested dielectric properties fall within the known sensing parameters (seen in Sections IV (A) through (C)).

V. CONCLUSION

A concept for liquid chemical identification was proposed and evaluated based on the shift in the resonant frequency of an applied UHF RFID chipped tag. There was a good correlation between the measured results with the presented sensor design in comparison to a standard dielectric identification system (SPEAG Dak 3.5 probe system) currently available on the market. To our best knowledge this is the first chipped passive UHF RFID sensor design for liquid identification and dielectric measurement capable of being utilized with a minimum of a 2 meter read range for both low and high permittivity liquid solutions.

If all values within an identification system are kept stable, effective permittivity can be calculated from the observed resonance frequency shift, and used to differentiate between chemical liquids within both 2 mm and 5 mm borosilicate glass containers at an accuracy of ± 0.834 relative permittivity and ± 0.050 S $\cdot$ m^{-1} conductivity when compared to a standard dielectric measurement system available on the market.

When used within a closed bottle system, this design can differentiate between hazardous chemicals without the need to open the bottle and experience exposure to hazardous vapors. Utilizing a single passive sensor design as well as a single UHF wideband RFID reader (to differentiate all organic liquids as tested); it is possible to determine the dielectric properties of liquid solutions (within the parameters of the calibration curve) without the need of bespoke equipment. It should be noted that the full range of liquid differentiation is aimed at laboratory utilization not for the general market as to detect the full range of dielectric constants (2 to 80 permittivity as shown here) would be outside of the allowable regional frequency regulations for EPC class 1 Gen 2 ISO18000-6C RFID. This is proposed as a cost effective and quick alternative for chemical identification without the need to invest in expensive dielectric testing systems in addition to expensive wideband readers.

For more practical use, this design could be easily tuned in the future to function at a single frequency for any specific liquid chemical as long as that chemical falls within the 2 to 80 permittivity range as described here. Therefore, this design could potentially be used to detect contamination within closed vessels as long as the dielectric changes are above the sensitivity of the described system. This sensor tag would be ideal for future 'smart' storage system integration within research facilities or hospitals requiring automatic chemical tracking, easy contamination and/ or chemical identification within large autonomous storage rooms requiring both hand-off and continuous readings via an integrated reader antenna. The tag could also be utilized in a tracking system for closed liquid containers (such as during manufacturing/shipping of hazardous chemicals) as the presented design is a compact antenna label with good read distances on glass (6 meters in air).

As previously stated, this design is not intended to replace what is currently available on the market, in terms of dielectric property measurements, but rather to present a cheap, easy to manufacture sensor alternative for liquid bulk identification within known parameters using only a single wideband UHF RFID reader antenna or for the detection of dielectric changes (such as contamination) within a liquid by utilizing a tuned version of this design to fit any ETSI band as needed.

REFERENCES

[1] *CDCEmergency Response Card*. Accessed: Jun. 06, 2018. [Online]. Available: https://www.cdc.gov/niosh/ershdb/emergencyresponsecard_29750029.html

[2] *Thermo Fisher Scientific Butanol Safety Data Sheet*. Accessed: Jun. 06, 2018. [Online]. Available: https://www.fishersci.com/shop

[3] A. P. Gregory and R. N. Clarke, "A review of RF and microwave techniques for dielectric measurements on polar liquids," *IEEE Trans. Dielectr. Electr. Insul.*, vol. 13, no. 4, pp. 727–743, Aug. 2006.

[4] V. S. Pranavsesh and P. Jain, "Study of effect of dielectric superstrate on resonance frequency of patch antenna and measurement of dielectric constant of superstrate," in *Proc. Int. Conf. Comput. Techn. Inf. Commun. Technol. (ICCTICT)*, New Delhi, India, Mar. 2016, pp. 575–579.

[5] A. J. Cole and P. R. Young, "Chipless liquid sensing using a slotted cylindrical resonator," *IEEE Sensors J.*, vol. 18, no. 1, pp. 149–156, Jan. 2018.

[6] P. S. Bansode, K. Makhija, S. A. Gangal, and R. C. Aiyer, "Non-destructive measurement of dielectric constant using a 2.4 GHz microstrip patch antenna," in *Proc. 2nd Int. Symp. Phys. Technol. Sensors (ISPTS)*, Pune, India, Mar. 2015, pp. 219–223.

[7] D. Mathur, S. K. Bhatnagar, and V. Sahula, "Nondestructive method for measuring dielectric constant of sheet materials," in *Proc. IEEE Region Conf. TENCON*, Bali, Indonesia, Nov. 2011, pp. 1105–1109.

[8] F. Costa *et al.*, "A depolarizing chipless RF label for dielectric permittivity sensing," *IEEE Microw. Wireless Compon. Lett.*, vol. 28, no. 5, pp. 371–373, May 2018.

[9] H. Lobato-Morales, A. Corona-Chávez, J. L. Olvera-Cervantes, R. A. Chávez-Pérez, and J. L. Medina-Monroy, "Wireless sensing of complex dielectric permittivity of liquids based on the RFID," *IEEE Trans. Microw. Theory Techn.*, vol. 62, no. 9, pp. 2160–2167, Sep. 2014.

[10] A. Lázaro *et al.*, "Chipless dielectric constant sensor for structural health testing," *IEEE Sensors J.*, vol. 18, no. 13, pp. 5576–5585, Jul. 2018.

[11] M. Abdolrazzaghi, M. Daneshmand, and A. K. Iyer, "Strongly enhanced sensitivity in planar microwave sensors based on metamaterial coupling," *IEEE Trans. Microw. Theory Techn.*, vol. 66, no. 4, pp. 1843–1855, Apr. 2018.

[12] *VoyanticTagformance Pro*. Accessed: Jun. 6, 2018. [Online]. Available: https://voyantic.com/tagformance

[13] *Higgs-3 Product Overview*. Accessed: May 25, 2017. [Online]. Available: http://www.alientechnology.com/products/ic/higgs-3

[14] S. Zuffanelli, P. Aguilà, G. Zamora, F. Paredes, F. Martín, and J. Bonache, "An impedance matching method for optical disc-based UHF-RFID tags," in *Proc. IEEE Int. Conf. RFID (IEEE RFID)*, Orlando, FL, USA, Apr. 2014, pp. 15–22.

[15] *CST-Dassault Systemes*. Accessed: Oct. 10, 2018. [Online]. Available: https://www.cst.com/

[16] *SPEAG Dak 3.5*. Accessed: Jun. 6, 2018. [Online]. Available: https://www.speag.com/products/dak/dak-dielectric-probe-systems/dak-3-5-200-mhz-20-ghz

[17] *Shell Chemicals Xylene Data Sheet*. Accessed: Jun. 6, 2018. [Online]. Available: https://www.shell.com/business-customers/chemicals/our-products/solvents-hydrocarbon/aromatic-solvents

[18] B. Abedian and K. N. Baker, "Temperature effects on the electrical conductivity of dielectric liquids," *IEEE Trans. Dielectr. Electr. Insul.*, vol. 15, no. 3, pp. 888–892, Jun. 2008.

Viktorija Makarovaite (S'18) received the B.Sc. degree in biology and biochemistry in 2010, the M.Sc. degree in medical technology (currently known as MLS) from Rush University, Chicago, USA, in 2012, and the M.Sc. degree in medical mycology from the University of Manchester, Manchester, U.K., in 2015. She is currently pursuing the Ph.D. degree in electrical engineering with a focus on sensor design for medical applications. She was an Associate Lecturer with the School of Engineering and Digital Arts, University of Kent, Canterbury, U.K. She holds board certification as a medical scientist (MLS generalist) with the ASCP since 2013. Her research interests include medical sensors, medical technology, biomedical engineering, RFID antennas, and new materials.

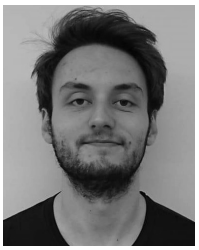

Aaron J. R. Hillier received the M.Sc. degree in forensic science from the University of Kent, Canterbury, U.K., in 2015, where he is currently pursuing the Ph.D. degree with the Communication Research Group and the Functional Materials Group, University of Kent. His current research interests include stimuli responsive polymers, passive sensing, and body-centric antennas.

Simon J. Holder received the Ph.D. degree in organic chemistry from the Liquid Crystal Group, University of Hull, in 1993, under the supervision of Dr. D. Lacey. After his Ph.D. degree, he went to work as a Post-Doctoral Research Fellow with the University of Kent on polysilane materials with Prof. Dick Jones and subsequently on supramolecular materials at the University of Nijmegen with Prof. R. Nolte. He was appointed as a Lecturer in Organic Chemistry at the University of Kent in 1999 and a Reader in Organic Chemistry in 2013. His current research projects include the development of materials for RFID sensors, novel polymer super-absorbents, and self-assembling block copolymers.

Campbell W. Gourlay received the Ph.D. degree in plant development from The John Innes Centre, where he studied the genetic control of leaf development. He began his career at The John Innes Centre in 1996. He is a Reader with the School of Biosciences, University of Kent. He established his own research group with the aid of Wellcome Trust Value in People Award and a Medical Research Council Career Development Fellowship in 2006. He is a Founding Member of the Kent Fungal Group, which represents one of the largest collections of yeast research groups in the U.K. His current research projects include: the regulation of mitochondrial health and the production of reactive oxygen species; the role of translational accuracy in healthy ageing and apoptosis; roles for the actin cytoskeleton in regulating stress response mechanisms; yeast as a model for motor neuron disease; using yeast to understand the development of multi-drug resistance; the role of mitochondrial function in the pathogenicity of *Candida albicans*; and the detection and management of biofilms on airway management devices.

John C. Batchelor (S'93–M'95–SM'07) received the B.Sc. and Ph.D. degrees from the University of Kent, Canterbury, U.K., in 1991 and 1995, respectively. From 1994 to 1996, he was a Research Assistant with the Electronics Department, University of Kent, where he became a Lecturer of Electronic Engineering in 1997. He is currently the Leader of the Antennas Group, University of Kent, and a Professor of Antenna Technology. His current research interests include UHF RFID tag design, passive sensing, body-centric antennas, printed antennas, compact multiband antennas, electromagnetic bandgap structures, and long-wavelength frequency selective surfaces.